Martensitic Transformation and Shape Memory Effect of NiCoMnSn High Temperature Shape Memory Alloy

F. Chen, Y. X. Tong, X. L. Lu, B. Tian, L. Li & Y. F. Zheng

Journal of Materials Engineering and Performance

ISSN 1059-9495
Volume 21
Number 12

J. of Materi Eng and Perform (2012)
21:2509-2514
DOI 10.1007/s11665-012-0371-4

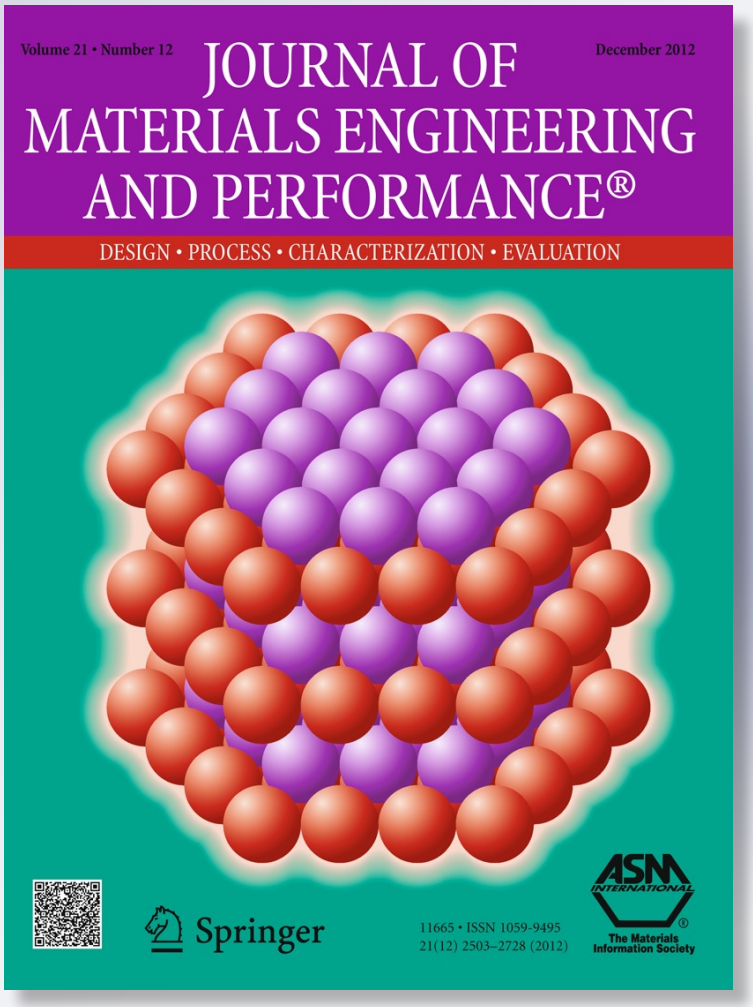

Springer

JMEPEG (2012) 21:2509–2514
DOI: 10.1007/s11665-012-0371-4

1059-9495/$19.00

Martensitic Transformation and Shape Memory Effect of NiCoMnSn High Temperature Shape Memory Alloy

F. Chen, Y.X. Tong, X.L. Lu, B. Tian, L. Li, and Y.F. Zheng

(Submitted February 22, 2012; in revised form June 27, 2012)

This article studies the dependence of martensitic transformation on Mn:Sn ratio in $Ni_{43}Co_7Mn_{50-x}Sn_x$ alloy and the shape memory behavior of $Ni_{43}Co_7Mn_{43}Sn_7$ in detail. The results show that all the transformation temperatures show a linear decrease with the decrease of Mn:Sn ratio. The similar tendency is also found in the change of T_c. $Ni_{43}Co_7Mn_{43}Sn_7$ alloy exhibits a moderate shape memory effect and the maximum shape recovery strain is 2.96%. Temperature memory effect is also observed in $Ni_{43}Co_7Mn_{43}Sn_7$ alloy.

Keywords high temperature, martensitic transformation, NiCoMnSn, shape memory alloy, shape recovery

1. Introduction

As an important subdivision of metamagnetic shape memory alloy (SMA), NiCoMnSn alloy is being attracting more and more attention. Just like NiCoMnIn, under a large enough external magnetic field, NiCoMnSn's transformation temperatures can be shifted down to low temperature (Ref 1). That is, magnetic-field-induced reverse transformation can occur in this alloy. Compared with NiCoMnIn, the latter has the advantage of low cost. Some scientists have carried out the investigations on martensitic behavior, microstructure, and magnetic property in NiCoMnSn alloys (Ref 2-7). Kainuma et al. reported a large magnetic-field-induced shape recovery strain of about 1.0% in a $Ni_{43}Co_7Mn_{39}Sn_{11}$ Heusler polycrystalline alloy (Ref 1). Ito et al. also found metamagnetic shape memory effect (SME), 0.56% recovery strain for the residual strain of 3.1% under the magnetic field of 8 T, in polycrystalline $Ni_{43}Co_7Mn_{39}Sn_{11}$ alloy fabricated by spark plasma sintering (Ref 2). Krenke et al. studied the effect of substitution of Co for Ni on martensitic behavior and inverse magnetocaloric properties in $Ni_{50}Mn_{37}Sn_{13}$ alloy. It is found that increasing Co concentrations causes the martensitic transition temperature to decrease, while the Curie temperature (T_c) increases. Moreover, the substitution by Co for Ni leads to a decrease in the magnetocaloric effect (Ref 3). The same phenomenon is also reported in Ref 4 and 5 in $Ni_{50-x}Co_xMn_{38}Sn_{12}$ and $Ni_{44-x}Co_xMn_{45}Sn_{11}$, respectively. In the case of Co substituting for Mn in $Ni_{43}Mn_{46-x}Co_xSn_{11}$ (x = 0-5) alloys, both martensitic transition temperature and T_c increase (Ref 6). For the alloy with x = 5, a large magnetic resistance of −59% are observed for the field change of 50 kOe at 281 K (Ref 6). These results indicate the Ni-Co-Mn-Sn ferromagnetic SMAs have great potential in magnetic refrigeration and magnetic sensor. All these studied NiCoMnSn alloys exhibit thermoelastic martensitic transformation near or below room temperature. However, the study on transformation behavior of NiCoMnSn based alloys at high temperature is seldom reported except for $Ni_{45}Co_5Mn_{40}Sn_{10}$ in Ref 7, which undergoes martensitic transformation at 135 °C.

Very recently, the present authors found that by changing the content of Mn and Sn on the basis of $Ni_{43}Co_7Mn_{39}Sn_{11}$, NiCoMnSn alloys also exhibit thermoelastic martensitic transformation at high temperature. That is to say, NiCoMnSn will be a candidate high temperature shape memory alloy (HTSMA). The martensitic transformation starting temperature (M_s) of $Ni_{43}Mn_{41}Co_7Sn_9$ alloy can reach up to 200 °C and its martensitic transformation was time-dependent (Ref 8). $Ni_{43}Mn_{43}Co_7Sn_7$ alloy undergoes a single-stage martensitic transformation and M_s is up to 288 °C (Ref 9). In order to make a good understanding of the martensitic transformation at high temperature and the effect of Mn:Sn ratio on martensitic transformation in NiCoMnSn alloy, the present paper makes Ni and Co content kept as 43 and 7, respectively, and Mn:Sn ratio is changed from 43:7 to 39:11. Furthermore, we focus on the martensitic transformation and shape recovery behavior of $Ni_{43}Co_7Mn_{43}Sn_7$ alloy.

2. Experimental Procedures

A series of alloys with the nominal compositions of $Ni_{43}Co_7Mn_{50-x}Sn_x$ (at.%) (x = 7, 8, 9, 10) were prepared by arc melting under an argon atmosphere using high-purity elements. Each button ingot was melted five times and cast into a chilled copper mold to obtain a master rod with a diameter of 10 mm and a length of 60 mm. The rods were sealed in quartz tubes under a

This article is an invited paper selected from presentations at the International Conference on Shape Memory and Superelastic Technologies 2011, held November 6-9, 2011, in Hong Kong, China, and has been expanded from the original presentation.

F. Chen, **Y.X. Tong**, **X.L. Lu**, **B. Tian**, and **L. Li**, Center for Biomedical Materials and Engineering, Harbin Engineering University, Harbin 150001, China; and **Y.F. Zheng**, Center for Biomedical Materials and Engineering, Harbin Engineering University, Harbin 150001, China and Department of Materials Science and Engineering, College of Engineering, Peking University, Beijing 100871, China. Contact e-mail: chenfeng01@hrbeu.edu.cn.

Table 1 Phase transformation temperatures and enthalpy change during the transformation from martensite to parent phase ($\Delta H_{M\text{-}P}$) of $Ni_{43}Co_7Mn_{50-x}Sn_x$ alloys (x = 7, 8, 9, 10)

Alloy	M_s, °C	M_f, °C	A_s, °C	A_f, °C	$\Delta H_{M\text{-}P}$, J/g
x = 7	288	242	268	303	29.87
x = 8	243	229	247	267	32.25
x = 9	193	180	193	209	24.64
x = 10	150	120	134	162	20.59

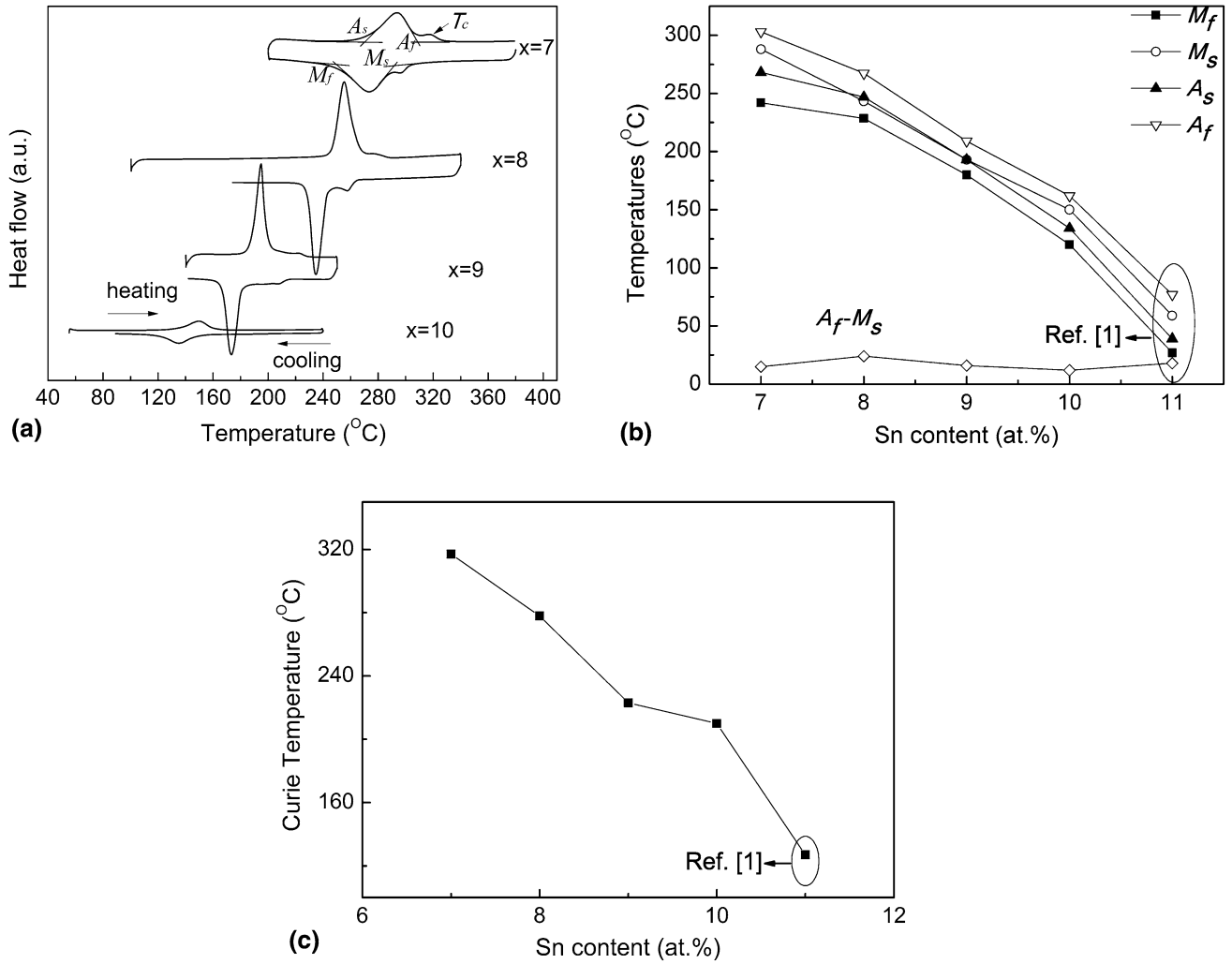

Fig. 1 (a) DSC curves. (b, c) The dependence of structural and magnetic transition temperatures on Sn content in $Ni_{43}Co_7Mn_{50-x}Sn_x$ alloys

vacuum and then annealed at 900 °C for 30 min followed by quenching into ice water for chemical homogeneity (Table 1).

The phase transformation behavior of the alloys was studied using a Perkin Elmer Diamond differential scanning calorimetry (DSC). The heating and cooling rate was 20 °C/min. The microstructure of the alloys was examined by optical microscope. The samples for optical observation were first mechanically polished and then etched in a solution of 99 mL C_2H_5OH + 2 mL HNO_3 + 5 g $FeCl_3$.

The compression tests were performed at room temperature (25 °C) on an Instron-3365 materials testing system at a crosshead displacement speed of 0.05 mm/min. The size of the samples for the compression test was 2 mm × 2 mm × 4 mm. The SME was measured using compression tests. In order to examine the SME, the samples were pre-compressed to a specific strain ε at room temperature and then heated by DSC to a temperature (400 °C) high enough for complete recovery. Residual strain after unloading is represented by ε_{re}, recovery strain during heating is represented by ε_R, which is marked by a curved arrow in the stress-strain curve. Shape recovery ratio (R) was calculated as $R = \varepsilon_R/\varepsilon_{re} \times 100\%$.

3. Results and Discussion

Figure 1 shows the DSC curves and the dependence of transformation temperatures as well as magnetic transition temperature on Sn content of $Ni_{43}Co_7Mn_{50-x}Sn_x$ (at.%) (x = 7, 8, 9, 10, 11) after annealing at 900 °C for 2 h. DSC results

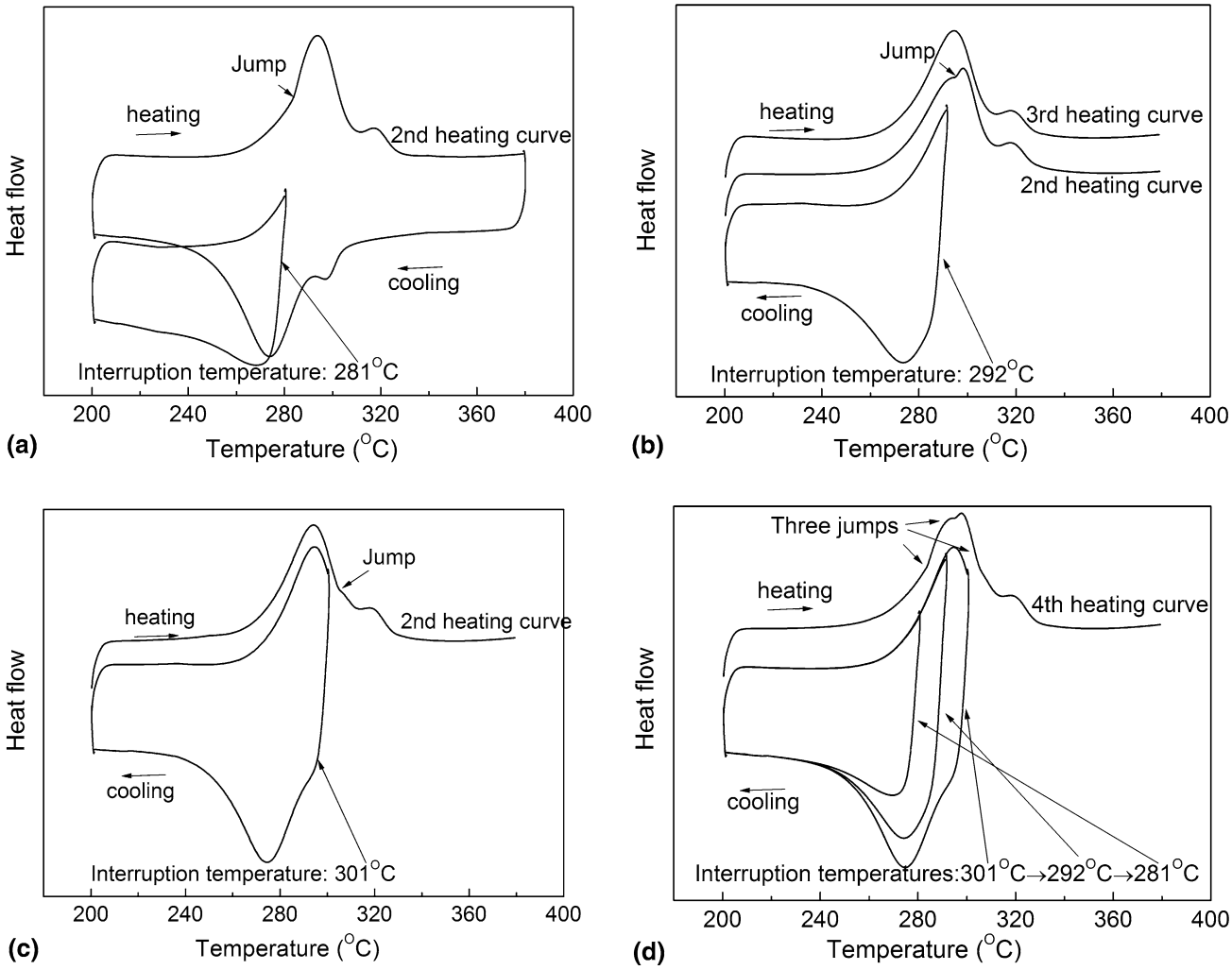

Fig. 2 DSC curves of $Ni_{43}Co_7Mn_{43}Sn_7$ alloy recording the effect of different thermal interruption temperature (T_i) on transformation behavior: (a) T_i = 281 °C; (b) T_i = 292 °C; (c) T_i = 301 °C; (d) T_i = three successive temperatures

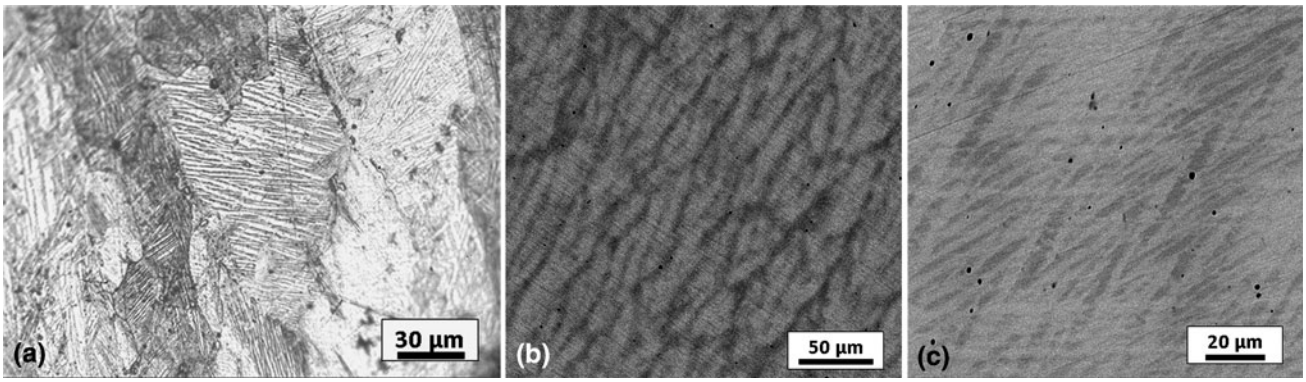

Fig. 3 (a, c) Optical and SEM images of as-annealed $Ni_{43}Co_7Mn_{43}Sn_7$ alloy (annealed at 900 °C for 1 h); (b) SEM image of as-cast $Ni_{43}Co_7Mn_{43}Sn_7$ alloy. (b, c) Backscattered electron images

show that, the change of the ratio of Mn to Sn has a remarkable effect on the structural and magnetic transition temperatures in NiCoMnSn alloy. For the annealed samples, single-stage martensitic and reverse transformation occurs upon cooling and heating, as shown in Fig. 1(a). Here A_s and A_f represent reverse transformation starting and finishing temperature, respectively, while M_f being martensitic transformation finishing temperature. The maximum thermal hysteresis (A_f-M_s) is about 20 °C indicating the present NiCoMnSn alloy undergoes a thermoelastic martensitic transformation. It is noted that, the fluctuation of (A_f-M_s) is very small. With the increase of Sn content, i.e., the decrease of Mn/Sn, all the transformation

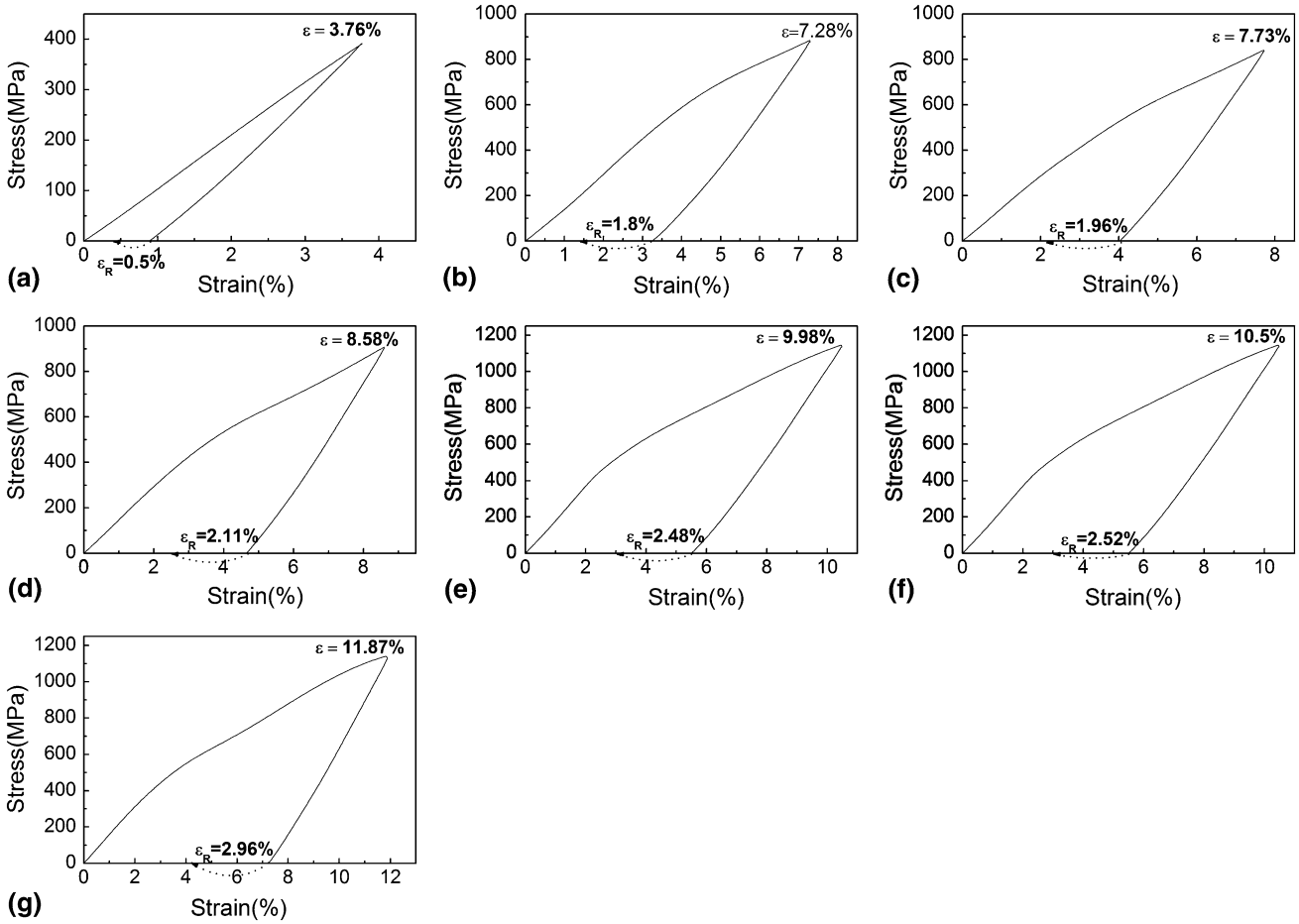

Fig. 4 The loading and unloading stress-strain curves of $Ni_{43}Co_7Mn_{43}Sn_7$ alloy under compression subjected to different strains, which are tested in the martensitic condition

temperatures show a linear decrease tendency (Fig. 1b). It is well known that the valence electron of Ni, Co, Mn, and Sn is 10, 9, 7, and 4, respectively. In the present paper, Ni and Co contents are kept constant. The decrease of Mn/Sn results in the decrease of electronic concentrations (e/a). Accordingly, the shift of M_s should be attributed to the decrease of e/a, which is the same as that reported in NiMnGa (Ref 10), NiMnSn (Ref 11), and NiMnIn (Ref 10) alloys. When Mn/Sn is 43:7, M_s is up to 288 °C. It is indicated that $Ni_{43}Co_7Mn_{43}Sn_7$ alloy is expected to be a promising high temperature SMA. While in the case of Mn/Sn being 39:11, M_s is dropped to 59 °C.

In addition, one small step is found after the reverse transformation and the other small step occurs before the martensitic transformation. According to Ref 1, 3, and 12, the former step corresponds to the magnetic transition of the parent phase during heating and the latter one is the magnetic transition of the parent phase during cooling. It should be noted that there exists a small hysteresis (about 20 °C) between these two steps, which is the same as that reported in other works (Ref 1, 12). However, the reason why the magnetic transition during cooling occurs at a lower temperature than that during heating is missing. For comparison easily, the step in the heating curve is used to represent T_c. While for $x = 8$, a small peak rather than a step occurs during cooling, which is against the characteristic of magnetic transition measured by DSC, as described above. Consequently, such a small peak upon cooling before the martensitic transformation may be due to the precursor phenomenon or pre-martensitic transformation. It is worth studying this phenomenon in the future. And the magnetic transition signal may be covered up by the pre-martensitic transformation.

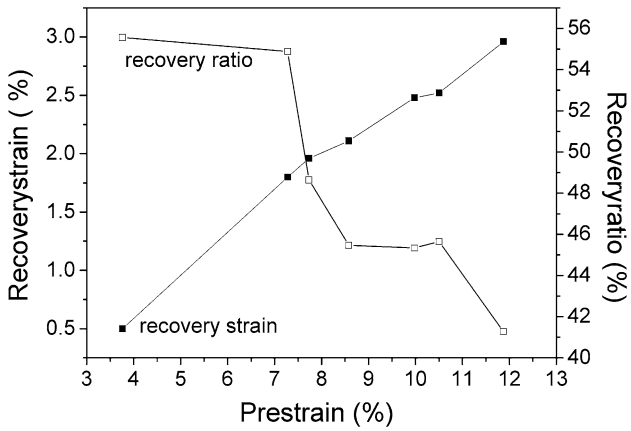

Fig. 5 Effect of pre-deformation on recovery strain and ratio of $Ni_{43}Co_7Mn_{43}Sn_7$ alloys

As shown in Fig. 1(c), the dependence of T_c on Sn content exhibits similar trend to transformation temperatures, which is due to the decrease of the total magnetic moment discussed in Ref 1).

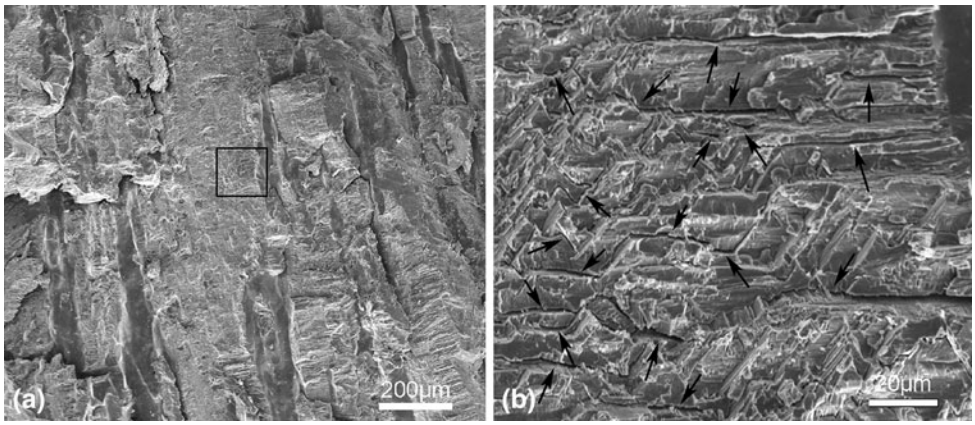

Fig. 6 SEM images of fracture surface in $Ni_{43}Co_7Mn_{43}Sn_7$ alloy, (b) is taken from the black rectangular area in (a)

Since the martensitic transformation in SMAs exhibits the thermoelastic characterization, SMAs are able to memorize their thermal history. That is, if the reverse transformation of a SMA is interrupted, a kinetic stop will appear in the next complete transformation (Ref 13). Some researchers called this phenomenon temperature memory effect (TME) or thermal arrest memory effect or step-wise martensite to austenite reversible transformation (Ref 13-15). The present authors used the name TME. To study TME in $Ni_{43}Co_7Mn_{43}Sn_7$ alloy, a thermal interruption is performed during heating using DSC and the detailed results are shown in Fig. 2. Here, thermal interruption means that the heating is temporarily stopped or arrested at a certain temperature between A_s and A_f, i.e., an incomplete reverse transformation is carried out. Subsequently, the sample is not followed by heating, but followed by cooling to the temperature below martensitic transformation finish temperature for completing a martensitic transformation. The detailed experimental procedure is as follows: (1) Heating from 200 °C, a temperature well below the M_f temperature, to an interruption temperature (T_i), a temperature within the temperature interval of the reverse transformation; (2) Holding for 1.0 min at T_i; (3) Cooling from T_i to 200 °C; (4) Heating from 200 °C to a temperature above A_f. During the second heating curve, an abnormal jump occurs, which disappears in the subsequent third heating curve. As shown in Fig. 2(a-c), an interruption corresponds to an abnormal jump, which appears at a temperature a little higher than T_i. In addition, as shown in Fig. 2(d), three interruptions correspond to three abnormal jumps, which occur not only at higher temperature than T_i but also in a certain sequence. That is to say, the alloy should remember the thermal history in the last time. This is the same as TME reported in NiTi (Ref 13, 14), whereas the effect is very weak for $Ni_{43}Co_7Mn_{43}Sn_7$ alloy. It is accepted that the elastic strain energy plays a role in TME. During an incomplete reverse transformation, some martensites change to the parent phase, the remaining martensite is called M1. Subsequent cooling down below M_f leads to martensitic transformation and the newly formed martensite is called M2. Due to the different formation mechanism, a lower elastic energy is stored in M1 than that in M2. As a result, the revere transformation starting temperature of M1 is a little higher than M2, which is the reason why TME occurs (Ref 13). The larger the difference of the elastic energy between M1 and M2, the more obvious the TME. As compared with NiTi alloy etc., the grain size of NiCoMnSn is much larger. This results in a relatively small amount of interface between M1 and M2, that is, the difference of the elastic strain energy between M1 and M2 is very small. Therefore the TME of NiCoMnSn is very weak.

The XRD patterns, which are not presented here, indicate $Ni_{43}Co_7Mn_{43}Sn_7$ alloy is a tetragonal structure martensite at room temperature. The optical image, as shown in Fig. 3(a) exhibits a typical martensite microstructure, self-accommodating martensite plate, which is in agreement with the XRD result. SEM images depicted in Fig. 3(b) and (c) show the effect of annealing treatment on microstructure. Figure 3(b) shows the micrograph of as-cast sample. It is clear that two morphologies exist, one with light contrast and the other with gray contrast, indicating that composition segregation exists in the as-cast sample. While for the as-annealed sample, as shown in Fig. 3(c), the difference of contrast caused by the segregation is not observed. Instead, the gray strips with different size are martensite plates with different orientation. The as-annealed sample is homogeneous in the chemical composition. The chemical homogeneity is greatly improved after annealing.

The compressive stress-strain curves of $Ni_{43}Co_7Mn_{43}Sn_7$ alloy subjected to different strains are measured, as shown in Fig. 4. It is shown that even when ε is 11%, the sample does not fracture. When ε is 3.76%, the shape recovery strain and ratio are 0.5 and 56%, respectively. With further deformation, the ε_{re} increases. The recovery strain and recovery ratio as a function of the pre-strain are shown in Fig. 5. It is seen that the recovery strain increase with increasing the pre-strain and reaches the maximum value of 2.96% when ε is 11.87%. As a whole, the recovery ratio shows an almost linear decrease from 56 to 41% with increasing pre-strain. It has been reported that the NiMnTi alloy shows a maximum shape recovery strain of 5% (Ref 16). The inferior SME in the present alloys possibly results from the fact that NiCoMnSn and NiMnTi alloys have different transformation mechanisms. In NiMnTi alloy, the transformation occurs between B2 parent phase and orthorhombic martensite (Ref 16). However, in the present alloys, the transformation occurs between B2 parent phase and tetragonal martensite. The transformation strain resulting from structural transition has an important effect on SME. Theoretically, the larger transformation strain, the larger SM effect. Due to the fact that transformation strain is smaller than that of NiMnTi, $Ni_{43}Co_7Mn_{43}Sn_7$ alloy exhibits a small recovery strain. In addition, in the real alloys, there are many other factors which affect the SM effect, such as the crystal defects, grain size, and the ductility. Especially for the NiCoMnSn alloy,

due to the weak grain boundary strength and large grain size, the sample often fractures along the grain boundary and exhibits very big brittleness, which is harmful to SM effect. Figure 6 shows the fracture morphology of $Ni_{43}Co_7Mn_{43}Sn_7$ alloy. Figure 6(a) exhibits a mixed feature of transgranular fracture and intergranular fracture. A considerable quantity of micro-cracks, as indicated by the arrows, are obviously observed in Fig. 6(b). SEM observations of the fracture surface indicates that this alloy is very brittle, which also goes against the SME. Therefore, $Ni_{43}Co_7Mn_{43}Sn_7$ polycrystalline sample studied here has an inferior SM effect and the maximum recovery strain is about 2.96%.

4. Conclusions

(1) The change of Mn/Sn has an obvious effect on transformation behavior of NiCoMnSn alloy. With the decrease of Mn/Sn, the transformation temperatures drop to low temperature, which is due to the decrease of e/a.
(2) A new type HTSMA, $Ni_{43}Co_7Mn_{43}Sn_7$, is presented in this paper. The maximum shape recovery strain is 2.96% and the recovery ratio decreases linearly with the increase of pre-strain.
(3) TME is observed in $Ni_{43}Co_7Mn_{43}Sn_7$ HTSMA.

Acknowledgments

The work was supported by the National Natural Science Foundation of China (51101040 and 51201044) and Harbin Special Fund for Innovation Talents of Science and Technology (2010RFQXG037).

References

1. R. Kainuma, Y. Imano, W. Ito, H. Morito, Y. Sutou, K. Oikawa, A. Fujita, K. Ishida, S. Okamoto, and O. Kitakami, Metamagnetic Shape Memory Effect in a Heusler-type $Ni_{43}Co_7Mn_{39}Sn_{11}$ Polycrystalline Alloy, *Appl. Phys. Lett.*, 2006, **8**(8), p 192513
2. K. Ito, W. Ito, R.Y. Umetsu, S. Tajima, H. Kawaura, R. Kainuma, and K. Ishida, Metamagnetic Shape Memory Effect in Polycrystalline NiCoMnSn Alloy Fabricated by Spark Plasma Sintering, *Scripta Mater.*, 2009, **61**, p 504–507
3. T. Krenke, E. Duman, M. Acet, X. Moya, L. Mañosa, and A. Planes, Effect of Co and Fe on the Inverse Magnetocaloric Properties of Ni-Mn-Sn, *J. Appl. Phys.*, 2007, **10**(2), p 033903
4. H.S. Liu, C.L. Zhang, Z.D. Han, H.C. Xuan, D.H. Wang, and Y.W. Du, The Effect of Co Doping on the Magnetic Entropy Changes in $Ni_{44-x}Co_xMn_{45}Sn_{11}$ Alloys, *J. Alloys. Compd.*, 2009, **467**, p 27–30
5. W. Ito, X. Xu, R.Y. Umetsu, T. Kanomata, K. Ishida, and R. Kainuma, Concentration Dependence of Magnetic Moment in $Ni_{50-x}Co_xMn_{50-y}Z_y$ (Z = In, Sn) Heusler Alloys, *Appl. Phys. Lett.*, 2010, **9**(7), p 242512
6. Z.D. Han, D. Wang, B. Qian, J.F. Feng, X.F. Jiang, and Y.W. Du, Phase Transitions, Magnetocaloric Effect and Magnetoresistance in Ni-Co-Mn-Sn Ferromagnetic Shape Memory Alloy, *Jpn. J. Appl. Phys.*, 2010, **49**, p 010211
7. V. Srivastava, X. Chen, and R.D. James, Hysteresis and Unusual Magnetic Properties in the Singular Heusler Alloy $Ni_{45}Co_5Mn_{40}Sn_{10}$, *Appl. Phys. Lett.*, 2010, **9**(7), p 014101
8. F. Chen, Y.X. Tong, B. Tian, Y.F. Zheng, and Y. Liu, Time Effect of Martensitic Transformation in $Ni_{43}Co_7Mn_{41}Sn_9$, *Intermetallics*, 2010, **18**, p 188–192
9. F. Chen, Y.X. Tong, B. Tian, L. Li, and Y.F. Zheng, Effect of Pre-strain on Martensitic Transformation of $Ni_{43}Mn_{43}Co_7Sn_7$ High Temperature Shape Memory Alloy, *Mater. Lett.*, 2010, **64**, p 1879–1882
10. X. Moya, L. Mañosa, A. Planes, T. Krenke, M. Acet, and E.F. Wassermann, Martensitic Transition and Magnetic Properties in Ni-Mn-X Alloys, *Mater. Sci. Eng., A*, 2006, **438–440**, p 911–915
11. V. Khovaylo, V. Koledov, V. Shavrov, M. Ohtsuka, H. Miki, T. Takagi, and V. Novosad, Influence of Cobalt on Phase Transitions in $Ni_{50}Mn_{37}Sn_{13}$, *Mater. Sci. Eng., A*, 2008, **481–482**, p 322–325
12. S. Besseghini, E. Villa, F. Passaretti, M. Pini, and F. Bonfanti, Plastic Deformation of NiMnGa Polycrystals, *Mater. Sci. Eng., A*, 2004, **378**, p 415–418
13. Y.J. Zheng, L.S. Cui, and J. Schrooten, Temperature Memory Effect of a Nickel-Titanium Shape Memory Alloy, *Appl. Phys. Lett.*, 2004, **84**, p 31–33
14. K. Madangopal, S. Banerjee, and S. Lele, Thermal Arrest Memory Effect, *Acta Metall. Mater.*, 1994, **42**, p 1875–1885
15. G. Airoldi, A. Corsi, and R. Riva, Step-wise Martensite to Austenite Reversible Transformation Stimulated by Temperature or Stress: A Comparison in NiTi Alloys, *Mater. Sci. Eng., A*, 1998, **241**, p 233–240
16. K.K. Jee, P.L. Potapov, S.Y. Song, and M.C. Shin, Shape Memory Effect in NiAl and NiMn-Based Alloy, *Scripta Mater.*, 1997, **36**, p 207–212